# Simulation Model of Electrical Steel Piercing

Sampsa V.A. Laakso[1*], Arijussi Väänänen[2], Sven Bossuyt[1] and Antero Arkkio[3]

[1]Department of Mechanical Engineering
Aalto University
Espoo, 02150, Finland

[2]Department of Materials Science and Engineering
Aalto University
Espoo, 02150, Finland

[3]Department of Electrical Engineering and Automation
Aalto University
Espoo, 02150, Finland

***ABSTRACT***

*Electrical steel is used for the active parts in electrical machinery that form the magnetic circuits because the material experiences low iron loss, and thus, has superior magnetizing properties. A typical electrical sheet has a thickness of 0.5 mm and is punched into its final shape via a piercing process. Piercing causes large deformations and residual stresses in the narrow zone of the cut surface. The deformations and stresses weaken the magnetic properties of the electrical sheet and result in additional losses, as the iron loss increases after piercing [1]. This paper presents a simulation model of the piercing process to evaluate the deformations and stresses on the cut surface. The model is constructed using the commercial FEM solver Deform. There has been an attempt to simulate the magneto-mechanical state of the punched surfaces, but the piercing process itself was not simulated [2]. The electrical steel sheet investigated in this paper is isotropic electrical silicon steel M400-50A (EN 10106-96).*

## 1. INTRODUCTION

Non-oriented electrical steels, such as M400-50A, are commonly used in rotating machines. The M400-50A designation reads as M for magnetising steel with maximum iron losses of 4 W/kg (400), 50 for a thickness of 0.5 mm and A for non-oriented grains. The iron losses in electrical steels can be divided into two main categories: hysteresis losses and dynamic losses. Dynamic losses can be further divided into classical losses and excess losses, which are significantly smaller than dynamic losses [3]. Piercing is a typical process for manufacturing electrical steel sheet parts. It results in good production output, relatively low production costs and consistent quality. However, the mechanical cutting of the sheet increases the iron losses in electrical steel, and therefore, it is important to minimise the deformations caused by the tool, especially since the standards set by the International Electrotechnical Commission (IEC) will have stricter limits regarding the energy efficiency of electromechanical machines in the near future, with an IE5 class efficiency that experts estimate will exceed the previous IE4 class (IEC 60034-30-1:2014) requirements by 20% [4,5]. To address this issue, simulation model of the piercing process is developed to investigate the effect of different tool and process parameters on the mechanical state of the cut surface. FEM simulations of blanking allows to predict edge quality, tool wear and forces, and the effect of the process parameters, but the quantitative accuracy of the simulations is strongly dependent on the modelling accuracy of the geometry and tool properties, such as the misalignment of the tool or tool deflections [6]. Ossart et al. (2000) developed a magneto-mechanistic model to describe the effect of plastic strain on the magnetic field and induction, both of which correlate quite well with the measured data [2].

## 2. MATERIALS AND METHODS

A material model for M400-50A steel is required to simulate the piercing process. The Hollomon model [7] for strain hardening and the Cockroft-Latham damage model [8] are selected for this study because both models are commonly used and not overly complex. Thermal softening and rate sensitivity are not considered in this study because it is assumed that their effect is negligible in the piercing process.

Hollomon model: $\sigma = K\varepsilon^m$,
Where $s$ = stress, $e$= strain, $K$ = yield stress equivalent, and $m$ = strain hardening exponent.

Cockroft-Latham model: $C = \int^{\varepsilon} \sigma^* d\varepsilon$,
Where $s$* = maximum principal stress and $C$ = critical value.

* Sampsa V.A. Laakso, DSc (Tech.): Tel.: +35840 70550 39; E-mail: sampsa.laakso@aalto.fi

The Hollomon parameters are acquired from tensile testing and the Cockroft-Latham parameters are acquired from shear testing using Digital Image Correlation and FEM simulations in the manner proposed by Tarigopula et al. 2008 [9]. The tensile tests are done using MTS Insight tensile testing equipment in both the rolling direction of the metal sheets as well as orthogonal to the rolling direction at a speed of 0.035 mm/s. The fitted Hollomon model, tensile test results and experimental set-up are shown in Figure 1. The shear test specimen modified according to recommendations by Tarigopula et al. is shown in Figure 2, but the geometry has been revised because the original experiment failed. The failure is caused by out-of-plane buckling of the test specimen, which thinner (0.5 mm) than the specimen proposed by Tarigopula et al. (1.5 mm). The resin coating on the steel sheets is removed with a NaOH solution at 100 °C. The geometry was machined with a wire EDM to avoid material deformation in the test specimen. The shear tests are done using MTS 858 tensile testing equipment and the LaVision DIC setup, as shown in Figure 2. The shear speed is set at 0.01 mm/s.

The shear tests and the piercing process are simulated using Deform FEM software from the Scientific Forming Technologies Corporation, and the results are compared to the testing results. The shear test simulation presented in Figure 3 are done using an elastic-plastic material model in the shear part and rigid ends of the specimen. The boundary conditions match the testing environment, thus allowing for free rotation around the pins. The workpiece is meshed with 43,820 tetrahedral elements. The piercing is simulated using the acquired material parameters. The Deform FEM software uses an updated Lagrangian formulation and a quasi-static implicit solver. The elements are linear quadratures with four integration points. The piercing process is modelled using an axisymmetric 2D simulation of punching a circular hole, shown in Figure 4. The outer diameter (157.5 mm) is matched with the outer diameter of the real punching tool since the diameter of the tool correlates with the punching force rather than with the punching area. Therefore, the radius of the punch tool is 25 mm. The workpiece is meshed with 12,593 square elements and the material model is elastic-plastic. The simulation are conducted using a Newton-Raphson iteration and skyline solver for a total of 400 steps, with $10^{-4}$ seconds per step.

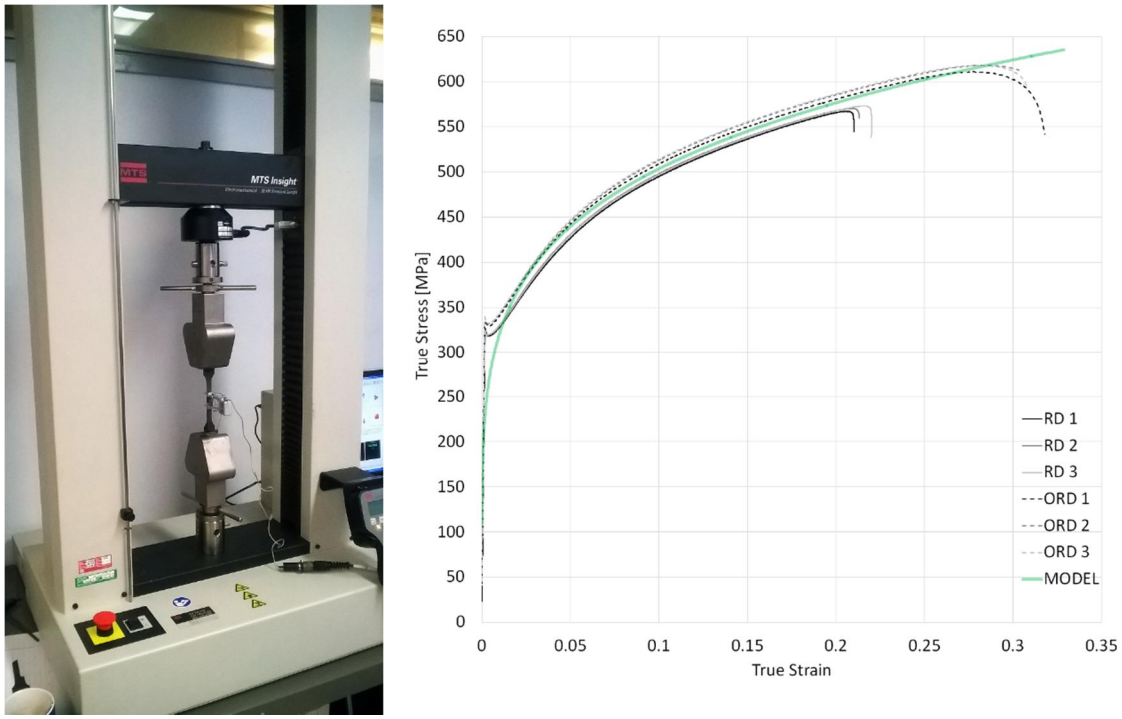


Figure 1: Tensile testing equipment and test results in the rolling direction (RD) and orthogonal to rolling direction (ORD).

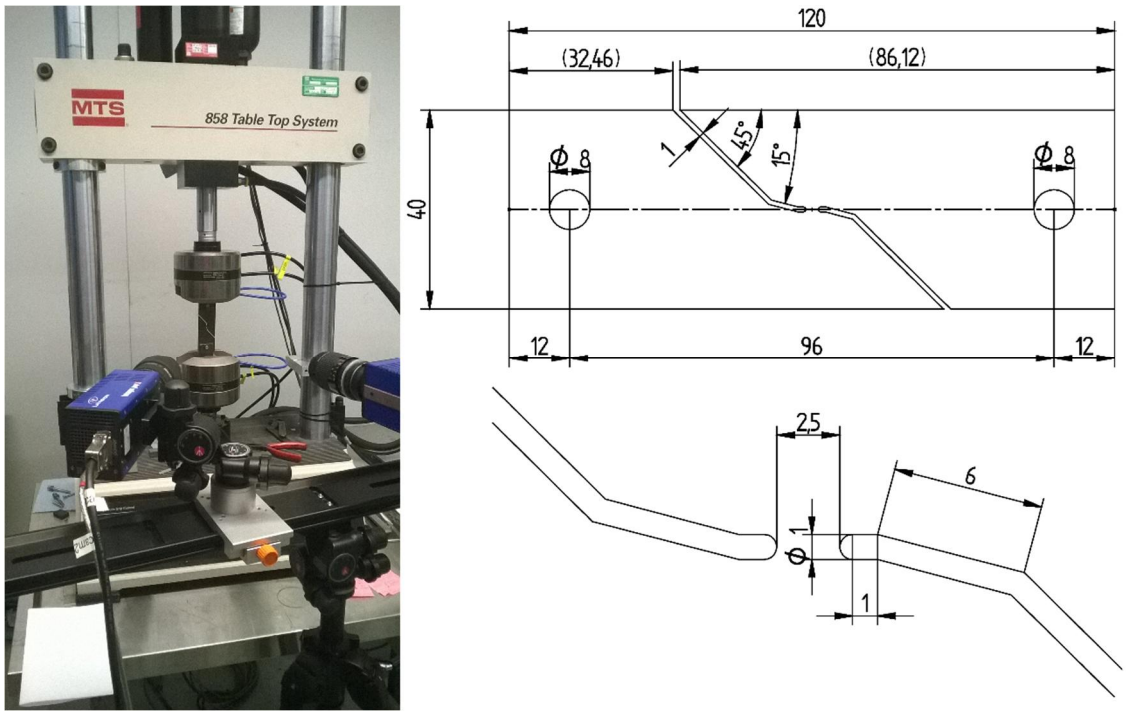


Figure 2: MTS 858 tensile testing equipment setup with the LaVision DIC cameras for shear strain measurement and shear test specimen modified according to recommendations by Tarigopula et al.

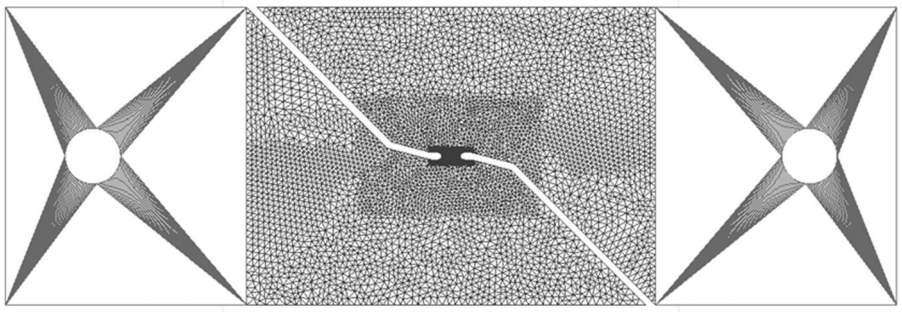

Figure 3: Shear test simulation setup.

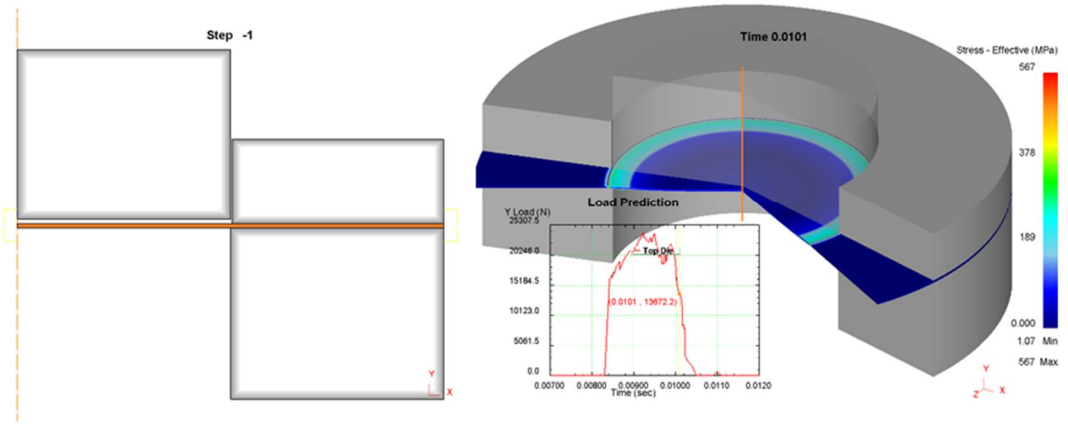


Figure 4: Axisymmetric 2D simulation setup for hole piercing.

## 3. RESULTS

The tensile testing results presented in Figure 1 show only a small variation in the stress-strain behaviour with different orientations. The stress is approximately 5% less in the rolling direction than in the orthogonal direction. It can be seen that the Hollomon equation, when fitted by minimising the absolute error, leads to a good fit, with an average error of 3%. The Hollomon parameters are K=789.6 and m=0.195. Figure 5 compares the shear test results with DIC to the simulated tests. The figure shows the simulations in the final configuration with respect to the damage parameters. The critical value, *C*, in the Cockroft-Latham model is calibrated by setting up the simulation with an estimated initial value (520). Then, the second set of simulations is conducted using a significantly larger value (800). Finally, final value (400) is calculated based on the difference between the time of fracture, shear force and shape of the strain field. Additionally, Figure 6 shows that the shear force from the experiments, simulations and curves are all in good agreement.

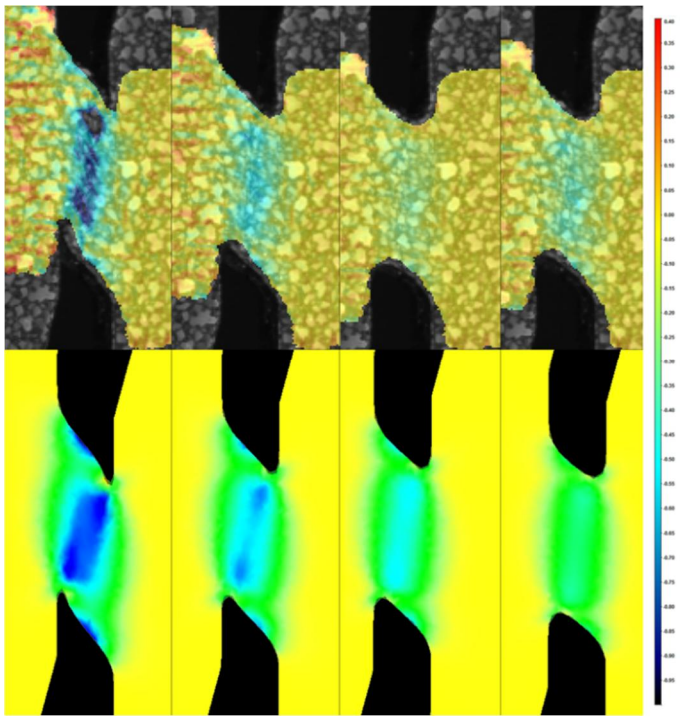

Figure 5: X-Y strains from DIC measurements and simulations at 140, 100, 80 and 60 seconds (the strain colorscale goes from red (0.4) to black (-1) at 0.05 intervals).

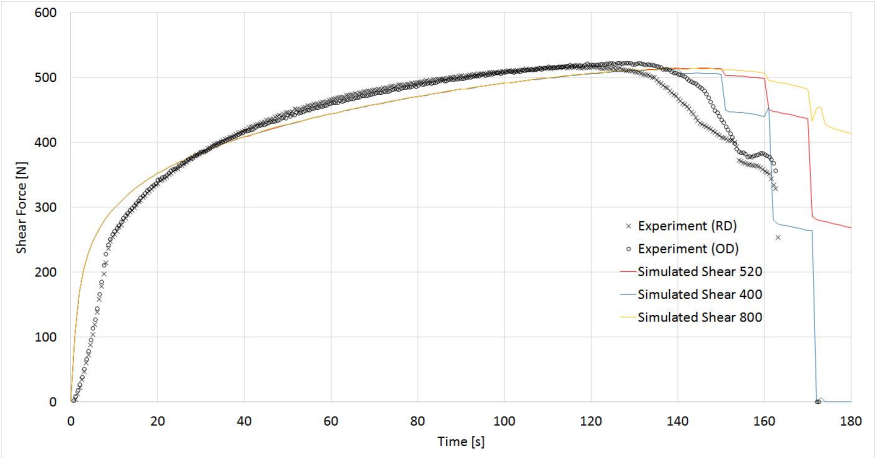


Figure 6: Shear force from simulations (red/blue/orange line) and experiments (black points) (the fracturing begins at 140 seconds).

The piecing simulation show compressive and shear stresses on the cut surface (±100 MPa). Compressive stresses are formed in the middle of the cut surface, peaking at approximately -100 MPa (light green area in Figure 7, left-hand side), and the stress continues through the workpiece for approximately 0.8 mm until it slopes down to a stress-free state. Shear stresses (orange and yellow areas) are formed on the top and bottom surfaces of the work, also peaking at approximately 100-150 MPa. First, the fracturing begins after the initial plastic deformation on the top of the workpiece. It then fractures from below, thus conforming to the generalised theory of the punching process.

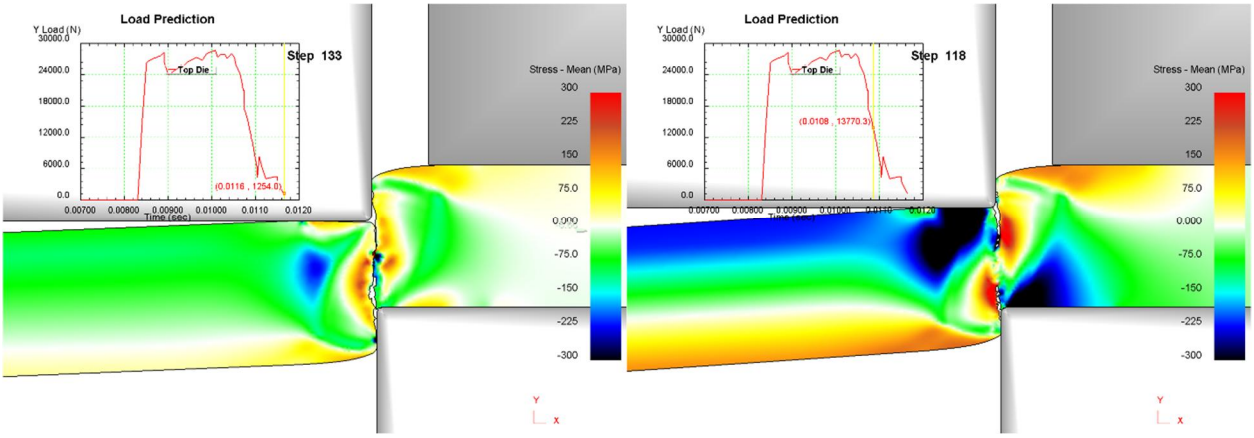


Figure 7: Simulated piercing after the fracture and during the middle of the fracturing process.

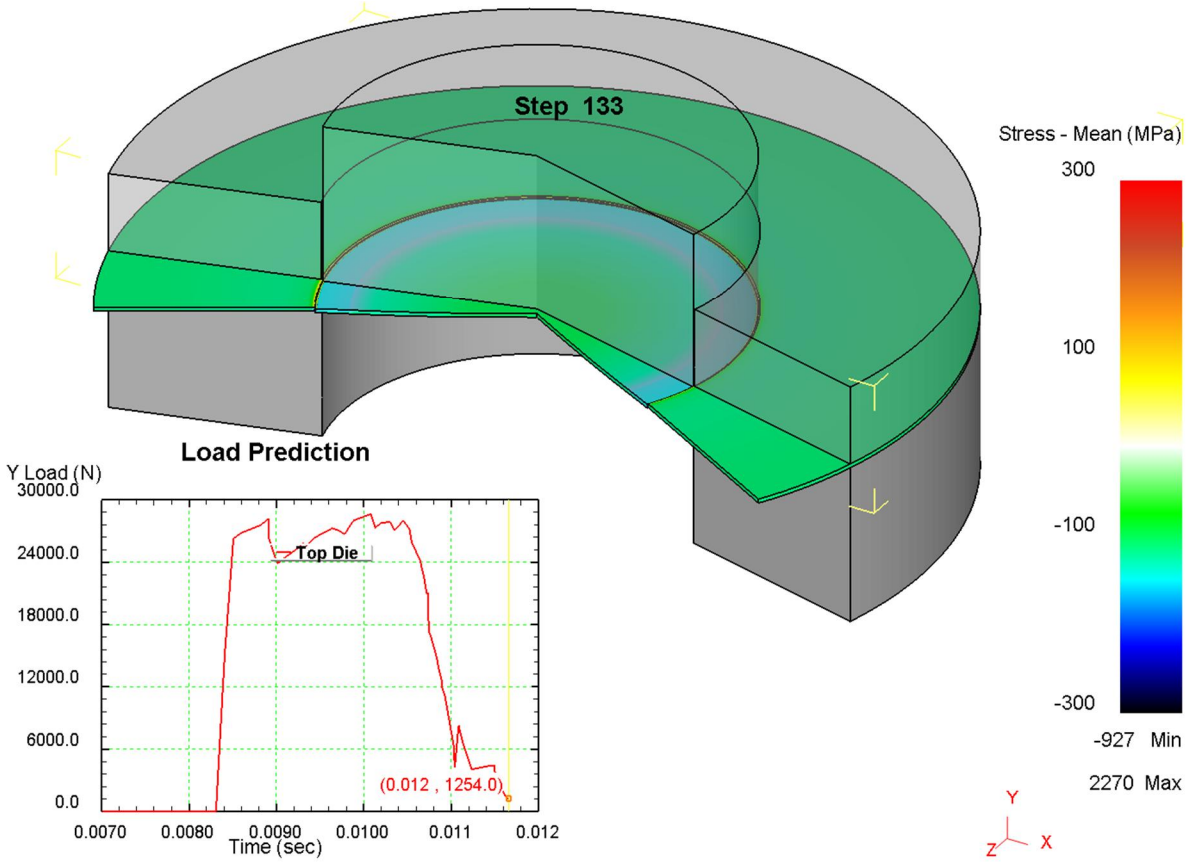


Figure 8: The simulation presented in 3D.

## 4. DISCUSSION AND CONCLUSIONS

This study demonstrates that simulations are a viable option for calculating the effect of tool and process parameters on the stress and strain when piercing electrical steel. The deformation contributes to iron losses, which in turn decrease the energy efficiency of electromechanical machines. The results presented in this paper indicate that the stress state in the workpiece is significant; indeed, previous studies have shown that it has a notable effect on iron losses in the material. In future research, the effect of deformation and residual stresses on iron losses can be simulated using the simulated deformation characteristics of the cut surface and electromagnetic FEM calculations. The effect of using a more detailed material model with thermal effects and rate sensitivity with respect to the accuracy of the simulations should be further investigated. The simulations can be verified by using a real pierced workpiece and micrographs of the cross-section of the cut surface. The deformations measured from the edge geometry of the workpiece can be used to evaluate total strain, whereas the microstructure can be used to evaluate the plastic strain to some extent.

## ACKNOWLEDGEMENTS

The authors would like to thank ABB Finland Oy and Dr Timo Holopainen for providing them with materials and their process knowledge on piercing.

## REFERENCES

*[1] Fujisaki, K.; Hirayama, R.; Kawachi, T.; Satou, S.; Kaidou, C.; Yabumoto, M.; Kubota, Takeshi, "Motor Core Iron Loss Analysis Evaluating Shrink Fitting and Stamping by Finite-Element Method," in Magnetics, IEEE Transactions on , vol.43, no.5, pp.1950-1954, May 2007*

*[2] Ossart, F.; Hug, E.; Hubert, O.; Buvat, C.; Billardon, Rene, "Effect of punching on electrical steels: Experimental and numerical coupled analysis," in Magnetics, IEEE Transactions on , vol.36, no.5, pp.3137-3140, Sep 2000*

*[3] Bertotti, Giorgio. "General properties of power losses in soft ferromagnetic materials." Magnetics, IEEE Transactions on 24.1 (1988): 621-630.*

*[4] ABB, Technical note; IEC 60034-30-1 standard on efficiency classes for low voltage AC motors,*

*https://library.e.abb.com/public/1018a82e36b29462c1257d41002b3470/TM025%20EN%2008-2014%20IEC60034-30-1_lowres.pdf, 2014*

*[5] Martin Doppelbauer, IEC Motor Efficiency Classes from IE1 to IE5, The Motor Summit China, Zhenjiang, Jiangsu province, China, 10-11 July 2015, http://www.motorsummit.ch/data/files/MS_2012/presentation/ms12_doppelbauer_update.pdf*

*[6] Altan, Taylan Tekkaya, A. Erman. (2012). Sheet Metal Forming - Processes and Applications - 1. Blanking. ASM International, http://app.knovel.com/hotlink/pdf/id:kt00AD2774/sheet-metal-forming-processes-2/blanking*

*[7] J. H. Hollomon, "Tensile deformation," Transaction of American Institute of Mechanical Engineering, vol. 162, pp. 268–277,1945*

*[8] Cockcroft MG, Latham DJ (1968) Ductility and the workability of metals. J Inst Met 96:33–39.*

*[9] Tarigopula, V., Hopperstad, O. S., Langseth, M., Clausen, A. H., Hild, F., Lademo, O. G., & Eriksson, M. (2008). A study of large plastic deformations in dual phase steel using digital image correlation and FE analysis. Experimental Mechanics, 48(2), 181-196.*